




Anomalous optical whispering-gallery mode induced by rotational symmetry breakingJin-hui Chen ^{1,2}, Wen Xiao,^{1,3} Sheng-ke Zhu,¹ Pei-Ji Zhang,² Qi-Tao Cao,²
Chao-fan Shen,¹ Cheng-Wei Qiu,^{3,*} Huanyang Chen ^{1,†} and Yun-Feng Xiao ^{2,4,‡}¹*Institute of Electromagnetics and Acoustics and Department of Physics,**College of Physical Science and Technology, Xiamen University, Xiamen 361005, China*²*State Key Laboratory for Mesoscopic Physics and Frontiers Science Center for Nano-optoelectronics,**School of Physics, Peking University, Beijing 100871, China*³*Department of Electrical and Computer Engineering, National University of Singapore, Singapore 117583, Singapore*⁴*Collaborative Innovation Center of Extreme Optics, Shanxi University, Taiyuan 030006, China*

(Received 5 July 2022; accepted 15 December 2023; published 16 January 2024)

We report that an anomalous optical whispering-gallery mode (WGM) emerges with self-focusing field patterns in a nearly spherical cavity of ultrahigh- Q factor, driven by rotational symmetry breaking and positive surface curvature. The positive Gaussian curvature modulates the evolution of light fields in the vicinity of a microsized surface, which is revealed by transformation optics theory. The geometry-induced self-focusing effect is resolved by the strongly confined field patterns of ultrahigh- Q modes. Furthermore, the nondiffracting interferometric field patterns with twist-chain-like profiles are observed by leveraging the degenerate-mode excitations in the surface of the microsphere cavity. The morphology-dependent WGMs can have potential applications in generating multiple orbital angular momentum beams when integrated with grating structures at the cavity surface. This work not only bridges the transformation optics and microcavity photonics in curved geometries but also provides a new route to on-chip optical field manipulation and light-matter interactions.

DOI: [10.1103/PhysRevA.109.013508](https://doi.org/10.1103/PhysRevA.109.013508)**I. INTRODUCTION**

Whispering-gallery-mode (WGM) microcavities confine light fields in a small volume for a long period of time, serving as a prominent platform for enhancing light-matter interactions. The past decades have witnessed the booming development of low-threshold microlasers, ultrasensitive sensors, efficient nonlinear optics, and cavity quantum optomechanics in WGM cavities [1–9]. Investigations into WGM microcavity optics have traditionally centered on the optical attributes inherent to bulk materials, such as the refractive index, absorption, thermal-optic effect, and optomechanical functions [3,4,10–12], for the proposed applications. Recently, photonic advances have ignited a substantial exploration of surface effects in WGM microcavities, for example, the second-order nonlinearity induced by surface symmetry breaking [9,13] and the strong spin-orbit coupling fields [14,15]. Notably, surface geometry plays a crucial role in the investigation of optics in curved space, inspired by general relativity. This field is fast emerging in the past years and has been instrumental in providing an experimental platform for the optical emulation of intriguing space-time phenomena [16–26]. Considering conventional WGM microcavities of a curved surface, nontrivial Gaussian curvature is expected to modulate the evolution of light fields in

the surface [21,23,27], although experimental observations remain elusive.

Microspheres, as the most fundamental three-dimensional WGM cavities, have been extensively studied for their robust ultrahigh- Q factors and the featured atomlike mode spectrum [1,9,28–30]. At a microsphere surface, the WGM fields can be solved from the vector Helmholtz equation via a separate variable method, and they are characterized by the angular momentum number l , azimuthal mode number m , and the transverse mode order p equals $l - m + 1$, i.e., the number of intensity maxima between the north and south poles [28,30]. When $l \gg 1$ and $l \sim m$, these WGM fields are confined in the equatorial area close to the cavity surface, akin to the light in a curved surface [21,23]. Due to the rotational symmetry of an ideal sphere, the azimuthal mode number is a good quantum number, resulting in a constant beam width along the azimuthal direction [Figs. 1(a) and 1(b)]. On the other hand, transformation optics exhibits a remarkable capacity for elucidating the behavior of light in curved surfaces. For example, the light field in a spherical surface can be emulated by a two-dimensional Maxwell's fish-eye lens based on the conformal coordinate transformation [27,31,32], and the latter can be further converted into one-dimensional (1D) Mikaelian lens (ML) by a simple exponential mapping [33,34]. In the scalar field approximation, WGMs of small transverse mode order can be emulated by the eigenstates of 1D ML [35], as shown in Fig. 1(c).

In this paper, we report that anomalous WGM fields with self-focusing patterns emerge in a slightly deformed microsphere surface, as shown in Figs. 1(d) and 1(e). These patterns

*chengwei.qiu@nus.edu.sg

†kenyon@xmu.edu.cn

‡yfxiao@pku.edu.cn

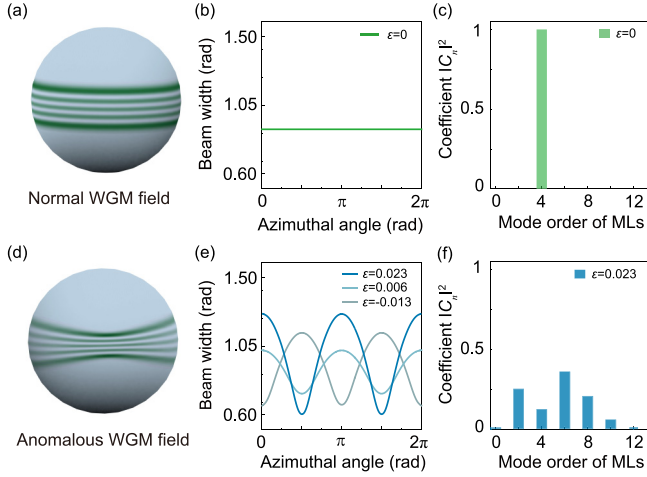


FIG. 1. (a) Schematic diagram of normal whispering-gallery-mode (WGM) field distributions in the surface of an ideal sphere cavity. (b) Constant beam width of normal WGM fields along the azimuthal direction. The radius of the sphere is set as $10 \mu\text{m}$. (c) Normal WGM is emulated by the eigenstate of the 1D Mikaelian lens (ML). (d) Schematic diagram of anomalous WGM fields with self-focusing in a deformed sphere cavity (ellipsoid). The term “anomalous” is to characterize the oscillating beam widths and the self-focusing effect of WGM fields. (e) Beam width of various anomalous WGM fields along the azimuthal direction. The axis radii of an ellipsoid are set as a_1, a_2, a_3 ($a_3 > a_1, a_2$), deformation $\varepsilon = (a_1 - a_2)/a_3$. The simulated structures of three typical ellipsoids are $(9.93, 9.7, 10) \mu\text{m}$, $(9.93, 9.87, 10) \mu\text{m}$, and $(9.8, 9.93, 10) \mu\text{m}$. Detailed simulations can be found in the Supplemental Material [35]. (f) Anomalous WGM is emulated by the superposition eigenstates of ML.

are driven by rotational symmetry breaking with inhomogeneous positive surface curvature, setting them apart from conventional WGMs. In the experiment, the self-focusing light field patterns of ultrahigh- Q WGMs in morphology-engineered microspheres are unambiguously demonstrated. In addition, complex light fields with the featured twist-chain-like distributions are observed, attributed to the interplay between the surface curvature and mode-interference effect. The morphology-dependent WGMs have potential applications for multiple orbital angular momentum (OAM) beam generation when the cavity surface is integrated with diffractive grating structures.

II. MODEL OF LIGHT FIELDS IN MICROSPHERE SURFACE

Without loss of generality, we first study the evolution of Hermite-Gaussian fields in a perfectly spherical surface emulated by the 1D ML in a flat x - y plane (x and y are Cartesian coordinate variables) by means of the transformation optics method [32,34]. Here, we suppose that Hermite-Gaussian fields,

$$\phi(x, y = 0) = \phi_0 H_n(2x/d_0) \exp(-2x^2/d_0^2), \quad (1)$$

are input into the ML $n_M = n_0/\cosh(x/R)$, where ϕ_0 is the optical field amplitude, $H_n(2x/d_0)$ is the n -order Hermite

polynomial, d_0 is the incident field width, n_0 is the background refractive index, and R is the surface radius of curvature. The propagating fields in the ML can be analytically solved with respect to the superposition of its eigenstates [35,36],

$$\psi(x, y) = \sum_{n=0}^{\infty} C_n (1 - \eta^2)^{\gamma/2} P_n^{(\gamma, \gamma)}(\eta) \exp(i\gamma y/R), \quad (2)$$

where

$$\gamma = [\sqrt{1 + 4(k_0 n_0 R)^2} - (2n + 1)]/2, \quad (3)$$

k_0 is the wave vector in vacuum, γ/R is the propagation constant of the n th mode, $\eta = \tanh(x/R)$, $P_n^{(\gamma, \gamma)}(\eta)$ is the normalized Jacobi polynomial, and C_n is the mode coefficient that can be calculated as

$$C_n = \int_{-\infty}^{+\infty} \phi(x, y = 0) \Omega_n^*(x) dx, \quad (4)$$

where $\Omega_n(x) = (1 - \eta^2)^{\gamma/2} P_n^{(\gamma, \gamma)}(\eta)$. Note that from Eq. (3), we have $k_0 n_0 R = \sqrt{(\gamma + n)(\gamma + n + 1)}$, which is exactly the resonant condition of WGMs in the surface if γ is an integer [27].

Based on the stereographic projection, the coordinates X, Y, Z on a spherical surface can be linked to a flat plane with the coordinate transformation [35], $X/R = \frac{2e^{x/R} \cos(y/R)}{1 + e^{2x/R}}$, $Y/R = \frac{2e^{x/R} \sin(y/R)}{1 + e^{2x/R}}$, $Z/R = \frac{e^{2x/R} - 1}{1 + e^{2x/R}}$, where X, Y, Z are Cartesian coordinate variables in three-dimensional space. Consequently, the evolution of Hermite-Gaussian optical fields in a spherical surface can be obtained from Eq. (2).

In particular, under the paraxial approximation, the analytical expression of the propagating Hermite-Gaussian fields of the fundamental mode can be derived through the coordinate transformation [35],

$$|\psi(\theta, \phi)|^2 = I_0 \frac{d_0}{\omega(\phi)} \exp\left(-\frac{4l_\theta^2}{\omega^2(\phi)}\right), \quad (5)$$

where $\omega(\phi) = d_0 \sqrt{\cos^2(\phi) + (2\alpha/d_0)^4 \sin^2(\phi)}$, $\alpha = \sqrt{R/(k_0 n_0)}$ is the characteristic length related to the surface radius of curvature (R), $l_\theta = R(\pi/2 - \theta)$, and ϕ and θ are the azimuthal and polar angles, respectively. Intriguingly, when the incident Hermite-Gaussian fields strictly satisfy the condition of $d_0 = 2\alpha$, the propagating field profile is constant, which accords with results via directly solving the Helmholtz equation in generalized coordinates [20,21]. We note that when the critical beam width and spectral resonance of light are simultaneously fulfilled, the conventional WGMs can be emulated by the eigenstates in 1D ML as shown in Fig. 1(c) [35]. In addition, when $d_0 > 2\alpha$ ($d_0 < 2\alpha$), the propagating fields in the sphere surface are self-focused (self-defocused) with an azimuthal period of π based on Eq. (5).

The self-focusing/defocusing effects of propagating fields regulated by the input beam width have been reported previously [21,23,27], which are driven by the positive constant surface curvature. Nevertheless, such anomalous WGMs with resonant spectral properties cannot be observed in a perfect sphere cavity. The eigenstates of the spherical cavity from the Helmholtz equation are unique, i.e., normal WGMs with propagation-invariant fields, which are protected by rotational

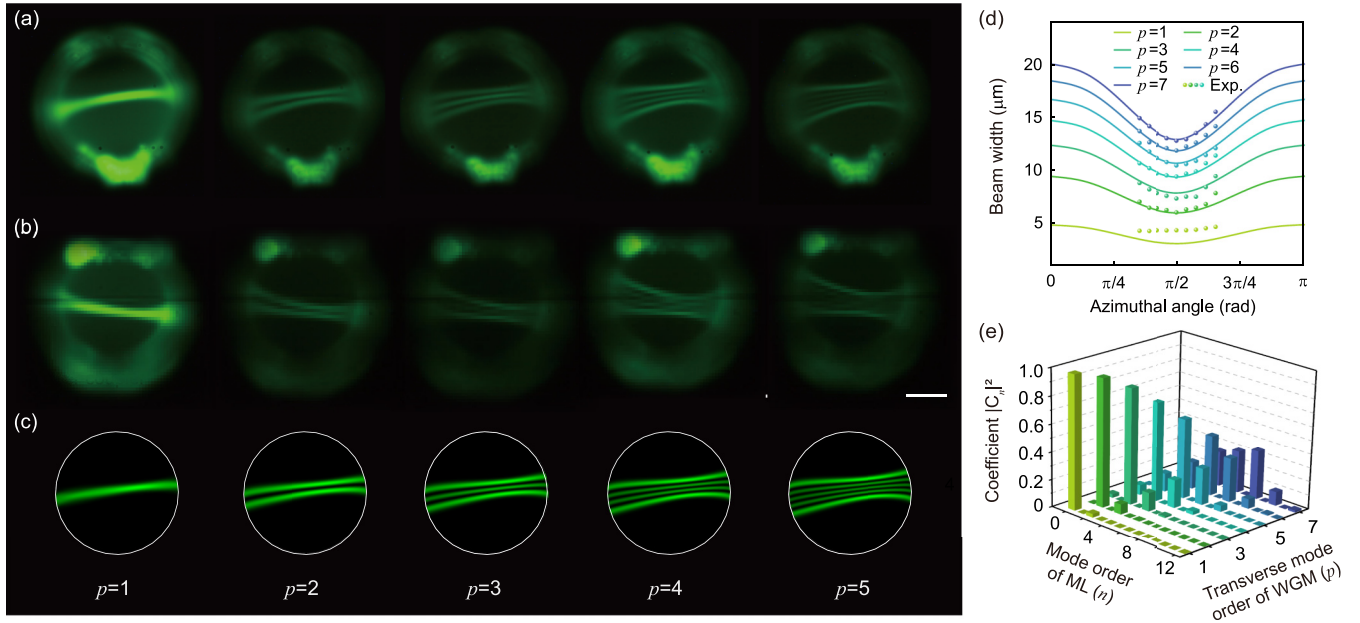


FIG. 2. Observation of anomalous WGM field patterns. Optical microscope images of anomalous WGM field patterns with self-focusing in a whole microsphere surface from (a) the front view and (b) the back view. The infrared pump light is input from a microfiber coupler. The optical fields with various transverse mode orders ($p = 1-5$) are excited by simply tuning the pump light wavelength and the fiber coupler positions. The scale bar is $20 \mu\text{m}$. (c) Analytical results of anomalous WGM fields in the microsphere surface based on transformation optics theory. (d) Measured and calculated beam width of anomalous WGM fields with transverse mode order p in the range of 1–7. (e) Anomalous WGM fields emulated by superposition of the eigenstates in ML.

symmetry. Here, we show that by simply breaking the rotational symmetry of a spherical cavity, for example, using an ellipsoid, the resonant anomalous WGMs of high- Q factors can be achieved as shown in Figs. 1(d) and 1(e). These anomalous WGMs can be emulated by the superposition of eigenstates in 1D ML [35], as shown in Fig. 1(f). We also conduct numerical simulations of eigenstates of three-dimensional ellipsoids in COMSOL MULTIPHYSICS, and their self-focusing properties are clearly verified [35].

III. EXPERIMENTS OF ANOMALOUS WGM IN MICROSPHERE

In the experiment, a morphology-engineered silica microsphere with a diameter of $\sim 60 \mu\text{m}$ is fabricated and is further doped with erbium ions (Er^{3+}) in the surface [35,37,38]. The average Gaussian curvature of the microsphere cavity is approximately 3–5 orders of magnitude higher than that of previous work [21,23,27], therefore the curvature effect is significantly enhanced. The continuous tunable infrared laser source (CTL 1550, Toptica) is evanescently coupled into the Er^{3+} -doped microsphere cavity by a tapered fiber coupler. The microscope system is assembled for imaging the surface optical fields from different spatial views [35]. From the transmission spectra under weak input power, the resonant mode of the doped-microsphere shows an ultrahigh- Q factor of $\sim 1.1 \times 10^7$ [35], which can achieve strong light-matter interactions. The broadband transmission spectrum of the microsphere cavity can be used to estimate the structural deformations via the eccentricity-induced mode splitting [28,35]. Under a high pump power of the infrared laser, the Er^{3+} in the microsphere surface could convert coherent infrared light to broadband

incoherent green emission through the multiphoton absorption process, which is used for the direct optical imaging of infrared WGM field distributions.

The pump light is meticulously scanned within a wavelength range spanning from 1510 to 1570 nm to excite WGMs of different transverse mode orders (p). During this process, careful optimization of the tapered-fiber coupler's position is conducted to ensure efficient light coupling. In the microsphere surface, these anomalous WGM fields characterized by self-focusing patterns are unequivocally captured through the optical microscope system, as demonstrated in Figs. 2(a) and 2(b). This comprehensive imaging is performed from both frontside and backside views, offering a clear observation of these intriguing phenomena. With an increase of transverse mode order, the self-focusing effect of the optical fields is enhanced, which agrees well with the analytical results based on transformation optics theory, as shown in Fig. 2(c). Quantitatively, the extracted beam widths along the azimuthal direction from the measurements are also consistent with theoretical results as shown in Fig. 2(d). In view of the emulation by the superposition of eigenstates in ML, the higher the mode order is of anomalous WGM, the more diffuseness of the eigenstate components can be obtained as shown in Fig. 2(e). It is noteworthy that such resonant WGM fields with a self-focusing phenomenon induced by rotational symmetry breaking and positive surface curvature are experimentally observed. In addition, in the ultrahigh- Q microsphere cavity, the different orders of anomalous WGM fields can be directly excited in the near-field coupling configuration without any spatial modulators or photonic microstructures. We also fabricate various microsphere cavities with controlled morphology and measure their resonant field profiles [35]. The deformed

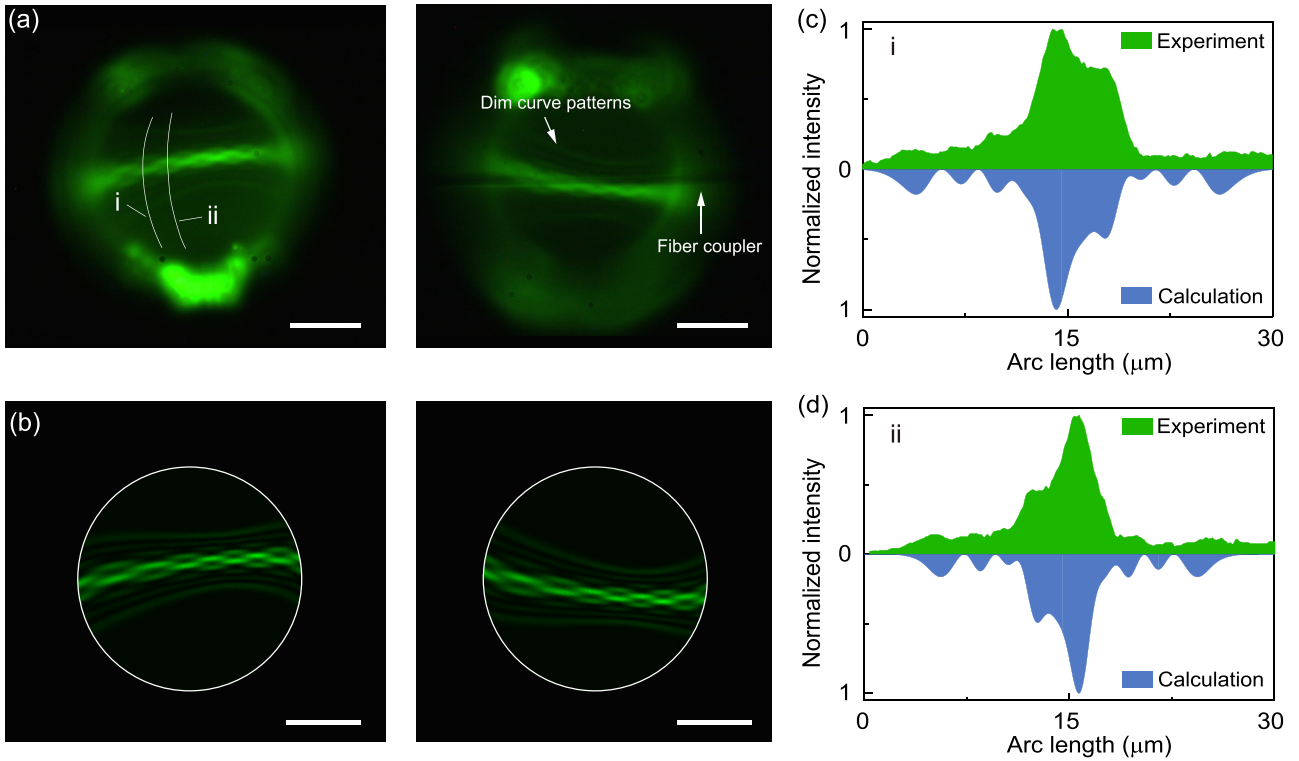


FIG. 3. Observation of nondiffracting mode-interference patterns at a full microsphere surface. (a) Optical microscope images of twist-chain-like field patterns in a microsphere surface from the frontside view (left panel) and backside view (right panel). (b) Analytical results of mode-interference patterns in the microsphere surface. The scale bar is 20 μm . Measured (green) and calculated (blue) optical field intensities at (c) curve line position i and (d) curve line position ii from (a), respectively.

microsphere cavity with rotational symmetry still supports normal WGMs, which accords with previous results [38,39]. In contrast, the microspheres of higher deformations along with rotational symmetry breaking show an enhanced self-focusing phenomenon as expected. We note that in order to clearly resolve these curving fields in the far-field regimes, the structural deformation-induced cross-sectional field deflection displacement should be larger than the optical diffraction limit, i.e., approximately half of the probe wavelength. For example, the calculated minimal deformation for observing these anomalous WGM is approximately 0.3% for a microsphere cavity of radius 10 μm .

When multiple anomalous WGMs of nearly degenerate resonant frequency are simultaneously excited in a microsphere surface, fascinating mode-interference patterns can be constructed. In the experiment, the infrared pump wavelength and fiber coupler position are finely tuned to realize simultaneous two-mode excitations and unconventional field patterns as shown in Fig. 3(a). The nondiffracting twist-chain-like fields along the equatorial circle are clearly imaged and accompanied by dim curved patterns. These complex mode-interference patterns can be emulated in the framework of ML, by two interferometric Hermite-Gaussian fields in the fundamental mode and ninth-order mode, respectively [35]. Based on the transformation, the theoretical results of propagating optical fields in the spherical surface are shown in Fig. 3(b). Note that the first focusing spot [Fig. 3(b), left panel] is not physically equal to the second one [Fig. 3(b), right panel] for their phase difference [35]. Quantitatively, we extract two

typical cross-section fields in the neighboring twist chains in Figs. 3(c) and 3(d), which are in good agreement with the calculations. We also conduct the numerical simulations of an ellipsoid cavity via the finite-difference time domain (FDTD) method, and similar multimode-interference patterns are obtained [35]. Thus by tailoring the optical excitations in a morphology-engineered microsphere, we can construct remarkably diversified optical fields in the microsphere surface, and this strategy can be readily applied to various curved microcavities.

IV. APPLICATION OF ANOMALOUS WGM

The morphology-dependent WGMs can have numerous potential applications such as optical coupling and sensing. Here, we propose that a deformed spherical cavity with self-focusing WGMs can be used to control the radiating OAM beams, as shown in Fig. 4(a). Supposing that diffracting grating structures are integrated in the surface of a spherical cavity at the equatorial plane, under the phase-matching conditions, the OAM beam can be radiated into free space [35,40]. A spheroid cavity with rotational symmetry can be used to generate OAM beams of high mode purity. In contrast, an ellipsoid cavity without rotational symmetry can be used to create multiple OAM beams [Fig. 4(b)], which have important applications in high-capacity information processing systems [41,42]. The mode purity of generated OAM beams by the spherical cavities is tunable by geometric deformations, as shown in Fig. 4(c). Thereafter, the morphology-dependent

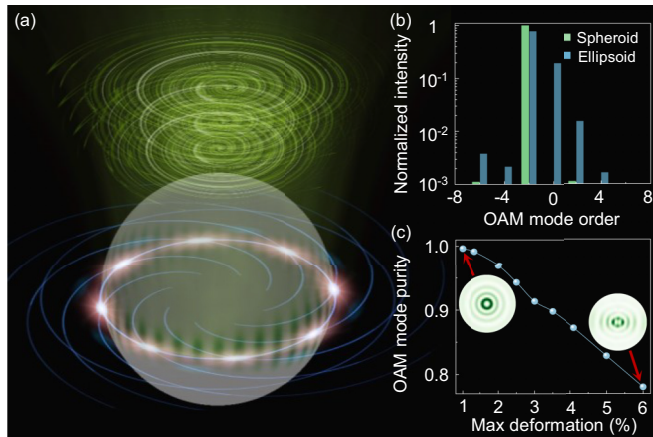


FIG. 4. Orbital angular momentum (OAM) beam emissions by the spherical cavity. (a) Schematic of radiating OAM in a deformed microsphere cavity with gratings along the surface of the equator. (b) The emitted left-handed circular polarization (LCP) OAM spectra from a spheroid cavity (with rotational symmetry) and an ellipsoid cavity (rotational symmetry breaking). The spheroid cavity is of the structural parameters (axis radius) $a_1 = a_2 = 4.95 \mu\text{m}$, $a_3 = 5 \mu\text{m}$. The ellipsoid cavity is of the structural parameters $a_1 = 4.7 \mu\text{m}$, $a_2 = 4.95 \mu\text{m}$, $a_3 = 5 \mu\text{m}$. The simulated WGM field is of $l = m = 24$, and the number of grating elements is 25. (c) Simulated LCP-OAM mode-purity change with the increase of structural deformations. The insets show the corresponding far-field patterns of radiated OAM beams.

WGMs in deformed spherical cavities provide a new route toward manipulating cavity OAM emission.

V. CONCLUSION

In summary, we have studied anomalous WGMs in ultrahigh- Q microsphere cavities with rotational symmetry breaking. Experimentally, we observe anomalous WGM fields with self-focusing driven by rotational symmetry breaking

and positive surface curvature. The intriguing twist-chain-like field patterns are obtained by leveraging degenerate-mode excitations in a morphology-engineered cavity, which unambiguously demonstrates the wave optics effect in the curved surface. Our work bridges the transformation optics and microcavity optics in curved geometries, and may provide a new paradigm for on-chip field manipulation and light-matter interactions [15,43]. Since the surface WGM fields play prominent functions in near-field coupling and optical sensing, the modulated WGM fields of a microcavity may spur innovative concepts in conventional cavity optics [2,44–46]. For example, the potential application for multiple OAM beam generation via anomalous WGMs is studied. In addition, the effect of surface curvature on WGMs can be used to develop sensitive optical measurements of shape deformations. It is worth emphasizing that the microcavity is an ideal platform for nonlinear optics [3,44], and the space curvature can serve as an additional dimension for modulating nonlinear effects such as the optical solitons in curved surfaces [20,47].

ACKNOWLEDGMENTS

We thank Prof. Lin Xu, Prof. Na Liu, Dr. Shijie Wang, Dr. Yangyang Zhou, and Dr. Xiangyang Wang for helpful discussions. This project was supported by the National Key R&D Program of China (2023YFA1407100), National Natural Science Foundation of China (Grants No. 12274357, No. 92050102, No. 62005231, No. 11825402, No. 92250302, No. 12174010, No. 12322411), Natural Science Foundation of Fujian Province of China (2023J06011, 2022J01064), and Fundamental Research Funds for the Central Universities (20720210045).

J.-h.C. and W.X. contributed equally to this work. J.-h.C. fabricated the device; J.-h.C., P.-J.Z., and C.-f.S. performed the experiment; J.-h.C., W.X., S.-k.Z., and H.C. built the theoretical model; J.-h.C., H.C., and Y.-F.X. organized the paper; H.C. conceived and supervised the theory; Y.-F.X. supervised the project; and all authors contributed to the discussion, analyzed the data, and wrote the manuscript.

- [1] K. J. Vahala, *Nature (London)* **424**, 839 (2003).
- [2] X. Jiang, A. J. Qavi, S. H. Huang, and L. Yang, *Matter* **3**, 371 (2020).
- [3] G. Lin, A. Coillet, and Y. K. Chembo, *Adv. Opt. Photonics* **9**, 828 (2017).
- [4] Y.-F. Xiao, C.-I. Zou, Q. Gong, and L. Yang, *Ultra-High-Q Optical Microcavities* (World Scientific, Singapore, 2020).
- [5] L. He, Ş. K. Özdemir, and L. Yang, *Laser Photonics Rev.* **7**, 60 (2013).
- [6] D.-Q. Yang, J.-H. Chen, Q.-T. Cao, B. Duan, H.-J. Chen, X.-C. Yu, and Y.-F. Xiao, *Light: Sci. Appl.* **10**, 128 (2021).
- [7] J.-H. Chen, X. Shen, S.-J. Tang, Q.-T. Cao, Q. Gong, and Y.-F. Xiao, *Phys. Rev. Lett.* **123**, 173902 (2019).
- [8] S.-J. Tang, P. H. Dannenberg, A. C. Liapis, N. Martino, Y. Zhuo, Y.-F. Xiao, and S.-H. Yun, *Light: Sci. Appl.* **10**, 23 (2021).
- [9] X. Zhang, Q.-T. Cao, Z. Wang, Y.-X. Liu, C.-W. Qiu, L. Yang, Q. Gong, and Y.-F. Xiao, *Nat. Photonics* **13**, 21 (2019).
- [10] A. Kovach, D. Chen, J. He, H. Choi, A. H. Dogan, M. Ghasemkhani, H. Taheri, and A. M. Armani, *Adv. Opt. Photonics* **12**, 135 (2020).
- [11] X. Jiang and L. Yang, *Light: Sci. Appl.* **9**, 24 (2020).
- [12] M. Aspelmeyer, T. J. Kippenberg, and F. Marquardt, *Rev. Mod. Phys.* **86**, 1391 (2014).
- [13] J. S. Levy, M. A. Foster, A. L. Gaeta, and M. Lipson, *Opt. Express* **19**, 11415 (2011).
- [14] C. Junge, D. O’Shea, J. Volz, and A. Rauschenbeutel, *Phys. Rev. Lett.* **110**, 213604 (2013).
- [15] P. Lodahl, S. Mahmoodian, S. Stobbe, A. Rauschenbeutel, P. Schneeweiss, J. Volz, H. Pichler, and P. Zoller, *Nature (London)* **541**, 473 (2017).
- [16] U. Leonhardt and T. G. Philbin, *New J. Phys.* **8**, 247 (2006).
- [17] D. A. Genov, S. Zhang, and X. Zhang, *Nat. Phys.* **5**, 687 (2009).
- [18] H. Chen, R.-X. Miao, and M. Li, *Opt. Express* **18**, 15183 (2010).

- [19] C. Sheng, H. Liu, Y. Wang, S. N. Zhu, and D. A. Genov, *Nat. Photonics* **7**, 902 (2013).
- [20] S. Batz and U. Peschel, *Phys. Rev. A* **78**, 043821 (2008).
- [21] V. H. Schultheiss, S. Batz, A. Szameit, F. Dreisow, S. Nolte, A. Tunnermann, S. Longhi, and U. Peschel, *Phys. Rev. Lett.* **105**, 143901 (2010).
- [22] C. Xu, A. Abbas, L.-G. Wang, S.-Y. Zhu, and M. S. Zubairy, *Phys. Rev. A* **97**, 063827 (2018).
- [23] V. H. Schultheiss, S. Batz, and U. Peschel, *Nat. Photonics* **10**, 106 (2016).
- [24] R. Bekenstein, Y. Kabessa, Y. Sharabi, O. Tal, N. Engheta, G. Eisenstein, A. J. Agranat, and M. Segev, *Nat. Photonics* **11**, 664 (2017).
- [25] R. Bekenstein, J. Nemirovsky, I. Kaminer, and M. Segev, *Phys. Rev. X* **4**, 011038 (2014).
- [26] A. Patsyk, M. A. Bandres, R. Bekenstein, and M. Segev, *Phys. Rev. X* **8**, 011001 (2018).
- [27] L. Xu, X. Wang, T. Tyc, C. Sheng, S. Zhu, H. Liu, and H. Chen, *Photonics Res.* **7**, 1266 (2019).
- [28] A. Chiasera, Y. Dumeige, P. Feron, M. Ferrari, Y. Jestin, G. N. Conti, S. Pelli, S. Soria, and G. C. Righini, *Laser Photonics Rev.* **4**, 457 (2010).
- [29] S. Spillane, T. Kippenberg, and K. Vahala, *Nature (London)* **415**, 621 (2002).
- [30] J. Kher-Alden, S. Maayani, L. L. Martin, M. Douvidzon, L. Deych, and T. Carmon, *Phys. Rev. X* **10**, 031049 (2020).
- [31] R. K. Luneburg, *Mathematical Theory of Optics* (University of California Press, Berkeley, 1964).
- [32] M. Šarbot and T. Tyc, *J. Opt.* **14**, 075705 (2012).
- [33] A. L. Mikaelian and A. M. Prokhorov, *Prog. Opt.* **17**, 279 (1980).
- [34] H. Chen, *Phys. Rev. A* **98**, 043843 (2018).
- [35] See Supplemental Material at <http://link.aps.org/supplemental/10.1103/PhysRevA.109.013508> for details.
- [36] X. Wang, H. Chen, H. Liu, L. Xu, C. Sheng, and S. Zhu, *Phys. Rev. Lett.* **119**, 033902 (2017).
- [37] S. Zhu, L. Shi, B. Xiao, X. Zhang, and X. Fan, *ACS Photonics* **5**, 3794 (2018).
- [38] L. Yang and K. Vahala, *Opt. Lett.* **28**, 592 (2003).
- [39] C. Dong, Y. Yang, Y. Shen, C. Zou, F. Sun, H. Ming, G. Guo, and Z. Han, *Opt. Commun.* **283**, 5117 (2010).
- [40] X. Cai, J. Wang, M. J. Strain, B. Johnson-Morris, J. Zhu, M. Sorel, J. L. O'Brien, M. G. Thompson, and S. Yu, *Science* **338**, 363 (2012).
- [41] X. Fang, H. Ren, K. Li, H. Luan, Y. Hua, Q. Zhang, X. Chen, and M. Gu, *Adv. Opt. Photonics* **13**, 772 (2021).
- [42] A. E. Willner, H. Huang, Y. Yan, Y. Ren, N. Ahmed, G. Xie, C. Bao, L. Li, Y. Cao, Z. Zhao *et al.*, *Adv. Opt. Photonics* **7**, 66 (2015).
- [43] V. Ginis, P. Tassin, J. Danckaert, C. M. Soukoulis, and I. Veretennicoff, *New J. Phys.* **14**, 033007 (2012).
- [44] W. Liu, Y.-L. Chen, S.-J. Tang, F. Vollmer, and Y.-F. Xiao, *Nano Lett.* **21**, 1566 (2021).
- [45] L.-K. Chen, Y.-Z. Gu, Q.-T. Cao, Q. Gong, J. Wiersig, and Y.-F. Xiao, *Phys. Rev. Lett.* **123**, 173903 (2019).
- [46] M. R. Foreman, J. D. Swaim, and F. Vollmer, *Adv. Opt. Photonics* **7**, 168 (2015).
- [47] S. Batz and U. Peschel, *Phys. Rev. A* **81**, 053806 (2010).